





# Preliminary screening of Pioglitazone and Diosgenin novel combination for Alzheimer's disease

Sheik Mohammed<sup>1</sup>, Anuradha Nandhyala<sup>1</sup>, Narasimha Rao Gaddam<sup>1</sup> , Kalirajan Rajagopal<sup>2</sup>, Nagarjuna Palathoti<sup>2</sup> , Justin Antony<sup>1\*</sup>

<sup>1</sup>Department of Pharmacology, JSS College of Pharmacy, JSS Academy of Higher Education & Research, Ooty, India.

<sup>2</sup>Department of Pharmaceutical Chemistry, JSS College of Pharmacy, JSS Academy of Higher Education & Research, Ooty, India.

## ARTICLE HISTORY

Received on: 29/04/2023

Accepted on: 12/08/2023

Available Online: 20/09/2023

### Key words:

Alzheimer's disease,  
beta amyloid proteins,  
PPAR- $\gamma$ , neuroinflammation.

## ABSTRACT

The pathophysiology of Alzheimer's disease (AD) is a complex phenomenon which mediating through A $\beta$  plaque formation and neurofibrillary tangles. Since, last few decades preclinical and clinical research evidences strengthen the elucidation of underlying causes in disease progression. The ongoing studies are mainly focused to screen the potential clinical candidates which turndown the neurodegeneration or delaying in AD progression. Considering the complicated etiopathogenesis of AD, the therapies which target the multiple molecular pathways of AD is required to potentiate the treatment and which in turn regulates the AD related complications. Diosgenin (DG), a natural steroidal saponin which has proven for an antioxidant, neuroprotective effects, and Pioglitazone is a peroxisome proliferator-activated receptor- $\gamma$  agonist that has been found to be effective in treating several neuropathies. DG and Pioglitazone combination may be a successful novel approach in treating AD and other neurodegenerative disorders; in the present study, we were targeted the neuro-inflammatory pathways with Pioglitazone and DG to evaluate the neuroprotective potential especially in AD like condition. Overall, the research findings revealed the possible therapeutic benefits with novel combination and it was notably down-regulated the cytokine storm and A $\beta$  plaque formation.

## INTRODUCTION

Alzheimer's disease (AD), which is the most common type of dementia, is a progressive neurodegenerative disease, most frequently characterized by early memory loss and cognitive decline that can eventually alter behavior, speech, visuospatial orientation, and the motor system [1]. It is identified by the presence of amyloid beta plaques (A $\beta$ ), tau protein phosphorylation, and neurofibrillary tangles (NFTs) as well as shrinkage and dysfunction of neuronal cells, which eventually leads to progressive cognitive, behavioral, and motor impairment and ultimately death [2]. The main factors that increase the likelihood of developing AD are age, genetic history, and apolipoprotein E4 (APOE4) genotype [3]. At present, 50 million people are affected by AD and prevalence will approach 152 million worldwide by 2050.

A $\beta$  was initially identified by sequencing amyloid plaques in the brains of AD and down syndrome patients [4]. They are formed from the protein called amyloid precursor protein (APP), which is sequentially cleaved by two enzymes:  $\beta$  and  $\gamma$  secretase. APP can be processed in nonamyloidogenic or amyloidogenic pathways. The A $\beta$  region is cleaved by  $\alpha$ -secretase as a result of nonamyloidogenic processing, preventing the formation of A $\beta$  [5]. In contrast,  $\beta$ -secretase cleavage of APP initiates amyloidogenic cleavage, which releases an amino-terminal ectodomain [6]. By cleaving the 99-residue carboxyl-terminal segment,  $\gamma$ -secretase generates A $\beta$  species comprising 38–43 residues [7]. Further evidence suggests about 10%–15% of early-onset familial AD cases are associated with APP mutations [8]. The Swedish mutation (APP<sup>Swe</sup>), one such mutations, is located at the cleavage site of  $\beta$ -secretase. This mutation accelerates  $\beta$ -cleavage, thereby enhancing the generation of all A $\beta$  species [9].

Apparently, there are no clinically promising solutions for these conditions. Diosgenin (DG), an eminent steroidal saponin that is widely distributed in medicinal herbs of

\*Corresponding Author

Justin Antony, Department of Pharmacology, JSS College of Pharmacy, JSS Academy of Higher Education & Research, Ooty, India.

E-mail: [justin@jssuni.edu.in](mailto:justin@jssuni.edu.in)

*Dioscorea* species is used as a principal source in producing steroidal medications [10]. It has received substantial attention for the prevention and treatment of various cancers [11], osteoporosis [12], cardiovascular diseases [13], atherosclerosis [14], diabetes mellitus (DM) [15], and skin conditions [16]. It is a light amorphous powder or white needle-shaped crystal with proven chemical and thermal stability under diverse environmental parameters [17]. The degree of DG's solubility in aqueous solutions is approximately 0.7 ng/ml [18].

As AD progresses, A $\beta$ -mediated chronic inflammation promotes microglia and astrocyte dysfunction, which in turn affects neuronal function and survival and eventually results in cognitive impairment [19]. In rat microglia and BV-2 cells induced with lipopolysaccharides, Wang *et al.* [20] discovered that DG significantly suppressed the production of proinflammatory factors such nitric oxide, Interleukin 6 (IL-6), and tumor necrosis factor (TNF)- $\alpha$ , thus achieving neuroprotective effects. Click here to enter text..

It has been observed that DG therapy dramatically reduced the cerebral cortex and hippocampal deposition of A $\beta$  plaques and NFTs. Furthermore, it lowered the quantity of axons and presynaptic terminals which had degenerated in the vicinity of amyloid plaques [21]. Research has shown that isolated DG may represent a new category of cognitive enhancers with essential activities that morphologically and functionally reinforce neuronal networks [22]. Also, in our earlier study, we have demonstrated the neuroprotective effect of DG (200 mg/kg/po) against A $\beta$  (1–42) induced neurotoxicity in animal model of AD. The mechanism of DG was attributed through attenuation of A $\beta$  (1–42) mediated plaque load, oxidative stress, and neuroinflammation [23]. In addition, acute and subchronic toxicity study on rats administered with DG orally at doses of 127.5, 255, and 510 mg/kg/day for 28 days did not show any significant toxicity signs in rats indicating the less toxicity of DG [24].

On the other hand, there is increasing evidence that complications caused by imbalances in insulin, particularly poor glucose tolerance and type II DM, elevate the probability of age-related cognitive decline and AD [25]. A $\beta$  deposits and an increase in tau hyperphosphorylation are two major causes of the neurodegeneration that develops in AD and are associated to be exacerbated by insulin resistance and peripheral hyperinsulinemia [26]. As a result, targeting insulin dysregulation could be a cutting-edge approach for the treatment of AD. Treatment with thiazolidinediones, agonists of the nuclear receptor peroxisome proliferator-activated receptor (PPAR- $\gamma$ ), such as Rosiglitazone and Pioglitazone, may be beneficial in the treatment of AD since they lower peripheral insulin and improve insulin sensitivity. Besides this, it has also been discovered that PPAR- $\gamma$  agonists have anti-inflammatory properties, regulate A $\beta$  homeostasis, and have neuroprotective potential [27].

Pioglitazone activates PPAR- $\gamma$  dependent peroxisome proliferator-activated receptor-gamma coactivator (PGC)-1 $\alpha$  co-activator signaling pathway and is found to be an effective strategy to exhibit neuroprotection in several neurodegenerative diseases [28].

Due to single targeting efficacy, many medicines for AD are failing to provide a successful therapy in Phase III clinical trials and even in pre-clinical investigations. This

clearly shows that the treatment of AD requires a multiple target strategy. To enhance cognitive functions in an AD-like condition, we therefore combined the synthetic drug Pioglitazone with the natural phytochemical DG to address numerous processes including excitotoxicity, neuroinflammation, oxidative stress, and mitochondrial dysfunction.

Pioglitazone that is already on the market would be combined with a novel cognitive enhancer, such as DG, and may be evaluated clinically based on pre-clinical results. Additionally, this combination can be advised for use in treating AD and other neurodegenerative diseases where excitotoxicity, neuroinflammation, oxidative stress, and mitochondrial dysfunction play a significant role in the onset and progression of disease. The new combination of Pioglitazone and DG's neuroprotective potential will be evaluated in appropriate *in silico* and *in vitro* models of AD.

## MATERIALS AND METHODOLOGY

### *In silico* studies

#### *ADMET prediction using swissADME and pkCSM online web tool*

To estimate the individual ADME behavior of the compounds DG and Pioglitazone, the Swiss Institute of Bioinformatics' Swiss ADME software ([www.swissadme.ch](http://www.swissadme.ch)) was accessed in a web server that displays the Swiss ADME Submission page in Google. A table was used to represent the outcomes for each input molecule [29].

#### *Pharmacokinetic properties*

The pkCSM tool was used to assess pharmacokinetic features. Smiles were collected from swissADME, and entered in the pkCSM tool, followed by a click on the ADMET button to receive comprehensive data.

#### *Optimum absorption*

Caco-2 cell permeability, an *in vitro* model was used for evaluating drug absorption in the human intestinal mucosa following oral administration. The permeability range of each molecule was classified using a prediction algorithm.

#### *Optimum distribution*

Gastrointestinal and brain penetration of derivatives/anacardic acids/peptide nucleic acid derivatives, were evaluated using the BOILED-Egg approach (brain or intestinal estimated permeation method). VDSS, known as volume of distribution, a theoretical volume that helps in the prediction of drugs total dose which could be necessary for a regular distribution to provide a concentration that is equivalent to the level found in plasma. The greater the VDSS value, the higher the drug distribution in tissue. If a molecule's log VDSS is less than 0.15, it is said to have low VDSS; if it is higher than 0.45, it is said to have high VDSS. Using pkCSM, the fraction unbound (Fu) value for each derivative/anacardic acid/polypeptide nucleic acid can be evaluated.

#### *Optimum of metabolism and excretion*

To determine excretion pathways, we subjectively assessed renal organic cation transporter 2 (OCT2) substrate

and quantitatively analyzed total clearance for all derivatives. Total clearance, that is the sum of renal and hepatic clearance, is quantified by a proportionality constant. By using the pkCSM tool, *in-silico* data on the metabolic properties of derivatives was examined to determine any potential safety concerns involving drug-drug interactions.

#### *Optimum toxicity*

Drug design and development are greatly simplified in the pharmaceutical industry by *in-silico* methodologies, which benefit the early detection of safety endpoints. The most frequently used quantifiable endpoints to screen out potential safety hazards include lethal rat acute toxicity (LD<sub>50</sub>), hERG inhibition, minnow toxicity, *Tetrahymena pyriformis* toxicity, and other significant toxicity endpoints. The use of pkCSM makes it simple to examine potential toxicity endpoints.

#### *Molecular docking*

The amino acids  $\beta$ -catenin (7AFW), PGC1- $\alpha$  (3CS8), GSK-3 $\beta$  (1Q4L), BACE-1 (4B05), JNK3 (4WH2), PPAR- $\gamma$  (2PRG) along with the existing cocrystals were obtained from Discovery Studio version 3.0 for active site prediction and to obtain the binding pockets. Molecular docking was performed for DG and Pioglitazone using the PyRx software to determine the target-ligand binding affinity and the root-mean-square deviation (RMSD) values. To facilitate molecular docking, PyRx has been utilized to ascertain the binding affinity of a ligand to a protein. The ligands were changed to protein data bank, partial charge (Q), and atom type (T) format following the devaluation. The macromolecule that will specify the binding site for the resulting protein was first selected. Following that, the active docking site was built using bound ligand binding locations. Then, all generated ligands were screened virtually on a molecular window, interacting with the specified active site [30,31]. The order of all ligands is then decided by their binding affinities as given by the PyRx score. The ligands were then divided into groups based on their binding energy levels.

#### *Molecular dynamics (MD)*

We performed a MD simulation using the Desmond module of Schrodinger 2020-1 to examine the atomic-level binding behavior of highly rated chemicals and to comprehend the molecular interaction analysis [32,33]. The ligand-protein complexes were positioned in single point charge water box for 10 minutes. To neutralize the charge, counter ions (33 Na<sup>+</sup> and 29 Cl<sup>-</sup> ions) were added. To mimic the physiological circumstances, salt level was fixed to 0.15 M sodium and chloride ions method. The short-range Vander Waals and Coulomb interactions were calculated at cut-off radius of 9.0 Å. A total of 100 ns MD simulation was performed with a timestep of 2 fs under an isothermal-isobaric ensemble (NPT) at a temperature of 300 K and pressure of 1 bar. OPLS-3e force field was employed in the simulations. Maestro's Desmond simulation interaction diagram tool was used to create plots and figures [34].

#### *In vitro model for AD*

##### *A $\beta$ <sub>25-35</sub> intoxicated SH-SY5Y cell culture*

A $\beta$ <sub>25-35</sub> was solubilized at 2.5 mM in 35% acetonitrile, 0.1% trifluoroacetic acid and diluted with double-distilled water

followed by phosphate-buffered saline (PBS) [35], yielding a 350 M stock solution. Three days were spent incubating the stock solution at 37°C, while pipetting the solution (50 strokes) every 3 days to aid in the production of large A $\beta$  aggregates. SH-SY5Y cell line was planted in a six-well plate in Dulbecco's modified eagle medium, supplemented with 10% fetal calf serum, penicillin (100 U/ml), and glutamine (0.3 mg/ml) and cultured at 37°C in a humidified tissue culture incubator containing 5% CO<sub>2</sub> [36]. Then, 10  $\mu$ M/l of synthetic coarse A $\beta$ <sub>25-35</sub> aggregates were added to the culture.

##### *3-(4,5-dimethylthiazol-2-yl)-2,5-diphenyl-2H-tetrazolium bromide (MTT) assay—cell viability*

The reduction of MTT to formazan will be used to assess neuronal viability in terms of mitochondrial metabolic performance. The cultured cells were intoxicated with A $\beta$ <sub>25-35</sub> and the combination of drugs was given with varying doses and exposure durations. After the removal of treatment, the cultured cells were washed in PBS and treated with MTT (5 mg/ml) in PBS for 2 hours at 37°C in 5% CO<sub>2</sub>. After several washings, the formazan crystals were dissolved in isopropanol and examined using spectrophotometer (570 nm, ref. 690 nm). The viability of the neurons was represented as a percentage of the control cells.

##### *Morphological observation*

Morphological changes were observed by using phase contrast microscopy to assess the degeneration and regeneration of neurons with respect to injury and treatment.

##### *Reactive oxygen species (ROS) assay—ROS expression*

The ROS test was done using 2',7'-dichlorodihydrofluorescein diacetate following drug treatment in the aforesaid intoxicated cell lines. After 24 hours of treatment, the cells were resuspended in a prewarmed PBS buffer containing a 10  $\mu$ M probe and incubated for 1 hour at 37°C. Fluorescence was measured with the fluorescence microplate reader with excitation at 495 nm and emission at 525 nm. The data were expressed as the percentage of cells that expressed dichlorofluorescein (DCF) intensity [37].

##### *Enzyme-linked immuno sorbent assay (ELISA)*

The cell lysates were separated and were subjected to estimate neuroinflammatory markers like IL-1 $\beta$ , TNF- $\alpha$ , etc., using respective ELISA kits as per manufacturer's instruction.

##### *Statistical analysis*

The results were expressed as mean  $\pm$  standard error of the mean. One-way analysis of variance has been used for the statistical analysis, followed by Tukey's multiple comparison using the software GraphPad Prism 9.0, where \*\*\* denotes the level of significance at  $p < 0.001$ .

## **RESULTS AND DISCUSSION**

### *In silico evaluation*

#### *ADME properties*

The swissADME and pkCSM webtool supports to analyze the biological activity as well as the drug likeness of the compound. It also has a major impact on the effectiveness of

**Table 1.** *In silico* ADME properties of DG and Pioglitazone.

Molecule	Formula	MW	#H-bond acceptors	#H-bond donors	MR	TPSA	iLOGP	#Lipinski violations
DG	C <sub>27</sub> H <sub>42</sub> O <sub>3</sub>	414.62	3	1	121.59	38.69	5.93	1
Pioglitazone	C <sub>19</sub> H <sub>20</sub> N <sub>2</sub> O <sub>3</sub> S	356.44	4	1	102.17	93.59	2.61	0

the bioactive molecules. The results of ADME prediction were mentioned in Table 2.

The characteristics of ADMET and MD were computed *in silico*. SwissADME and pkCSM have been employed to evaluate the drug-likeness and biological performance. As an outcome of the findings (Table 1), it was revealed that DG's log P value (iLog P 5.93) exceeded the Lipinski Rule of 5. It was taken into consideration since there weren't any other serious violations.

It was discovered using the boiled egg approach (Fig. 1) that Pioglitazone depicted good gastrointestinal absorption while DG exhibited promising blood-brain barrier (BBB) permeability.

### Docking results

The comparative *in silico* data of target proteins in AD was mentioned in Table 3.

### Docking analysis

*In silico* study results found that DG has greater binding affinity to BACE-1 when compared with the standard AZD3839 and docking score of DG was found to be -11.3 kcal/mol and for the standard AZD3839 -11.0 kcal/mol. AZD3839 is a known synthetic analogue that inhibits BACE-1.

Interactions of BACE-1 protein with the standard AZD3839 were found at positions Asp32, Leu30, Ile118, Gly230, Thr231, Ser35, Asn37, Trp76, Phe108, and Asp228, whereas DG has formed interaction at Trp115, Ile118, Ile110, Phe108, Arg128, Trp76, Val69, and Tyr71 positions in BACE-1 enzyme which was shown in Figures 2 and 3.

Pioglitazone docking score was noted -6.2 kcal/mol as shown in Table 3, whereas its standard agonist Rosiglitazone reported -5.2 kcal/mol and interactions has happened at Ile281, Tyr327, Ile341, Gln286, Ser289, Tyr473, Arg288, and Ser342 positions with PPAR- $\gamma$  as protein and Pioglitazone formed interactions in positions of Met329, Phe226, Ile326, Leu330, Arg288, Cys285, Phe363, His323, Ser289, and Gln286 as shown in Figures 4 and 5.

### MD simulation

MD simulation was done for the DG/4B05 complex to provide more insight into the structural forces for the antagonist binding affinity. The RMSD chart revealed that the BACE-1 enzyme complex (PDB ID 4B05) stabilized promptly after the simulation of 50 ns (Fig. 6). On the reference frame backbone, all frames from the 50 ns trajectory were aligned. A slight 0.14 Å variation in ligand RMSD was detected over the first 15 ns of the trajectory and in the last 10 ns of the trajectory, a 2.4 Å fluctuation in the plot was observed. However, this slight fluctuation in ligand had not undergone significant structural changes in ligand-protein complex because this variation is

**Table 2.** ADMET prediction of Pioglitazone and DG.

Model name	Predicted values	
	DG	Pioglitazone
Water solubility	-5.539 log mol/l	-4.309
Caco2 permeability	1.293 10 <sup>6</sup> cm/s	0.978
Intestinal absorption	96.565%	92.422
Skin Permeability	-3.39 log Kp	-2.705
P-glycoprotein substrate	No	No
P-glycoprotein I inhibitor	Yes	Yes
P-glycoprotein II inhibitor	Yes	Yes
VDss	0.426 log l/kg	-0.007
Fraction unbound	0 FU	0.017
BBB permeability	0.2 log BB	-0.591
CNS permeability	2.885 log PS	-2.496
CYP2D6 substrate	No	No
CYP3A4 substrate	Yes	Yes
CYP1A2 inhibitor	No	No
CYP2C19 inhibitor	No	Yes
CYP2C9 inhibitor	No	No
CYP2D6 inhibitor	No	No
CYP3A4 inhibitor	No	No
Total clearance	0.328 log ml/ minute/kg	-0.044 log ml/ minute/kg
Renal OCT2 substrate	No	No
AMES toxicity	No	No
Max. tolerated dose	-0.559	0.41
hERG I inhibitor	No	No
hERG II inhibitor	Yes	No
Oral Rat Acute Toxicity (LD <sub>50</sub> )	1.921 Mol/kg	2.258
Oral Rat Chronic Toxicity (LOAEL)	1.452 log mg/kg	1.379 log mg/kg
Hepatotoxicity	No	Yes
Skin sensitization	No	No
<i>T. pyriformis</i> toxicity	0.399 log ug/l	1.138 log ug/l
Minnnow toxicity	0.247 log Mm	0.094 log Mm

within the acceptable range of 1–3 Å. The interaction of DG with enzyme BACE-1 during MD simulation was represented in Figure 7.

### *In vitro* analysis

#### MTT assay

#### Individual assay

In this study, three test compounds to determine the cytotoxic impact on SH-SY5Y cells were tested. The test

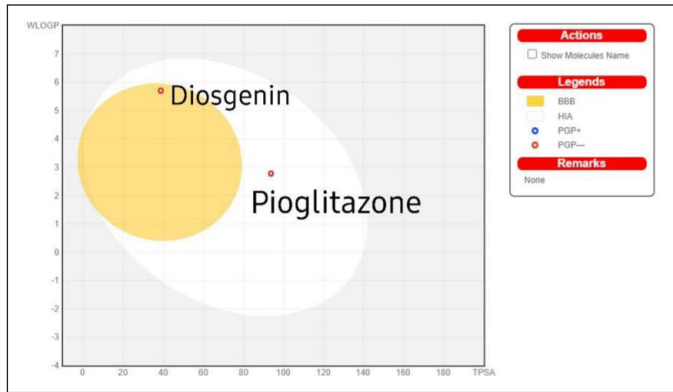


Figure 1. Boiled Egg approach.

Table 3. Comparative *in silico* data of target proteins in Alzheimer’s disease.

S. No	Target	PDB ID	Binding affinity (kcal/mol)		
			Standard	DG	Pioglitazone
1.	$\beta$ -catenin/Wnt signaling	7AFW	-6.3	-5.3	-6.0
2.	PGC1- $\alpha$	3CS8	-5.9	-4.3	-6.2
3.	GSK-3 $\beta$	1Q4L	-9.5	-8.3	-6.8
4.	BACE-1	4B05	-10.9	-11.3	-9.0
5.	JNK3	4WH2	-9.4	-8.3	-7.8
6.	PPAR- $\gamma$	2PRG	-8.5	-2.3	-9.4

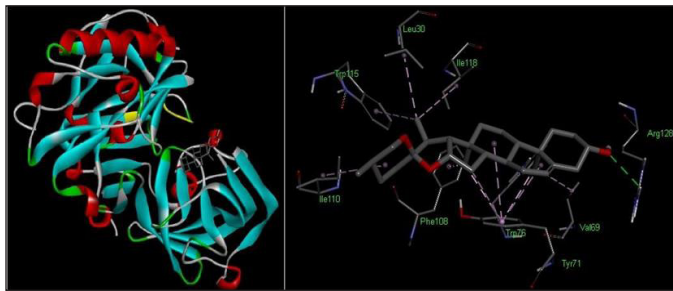


Figure 2. Docking model of 3-D crystallographic structure of BACE-1 against DG.

chemicals were then used to treat the cells that had the following concentrations as given in Table 4.

Observation

- The results of MTT assay show that the test chemicals, viz., Pioglitazone (Fig. 8) was cell-proliferative and noncytotoxic in nature and other compound, viz., DG (Fig. 9) moderately cytotoxic in nature on human bone marrow neuroblastoma (SH-SY5Y) cells with 65% cell viability at 100  $\mu$ M/ml concentration used for the study.
- The combination of these two compounds at 1:1 ratio also exhibited effective cell proliferation with 94.5% cell viability at the 100  $\mu$ M/ml concentration (Fig. 10).

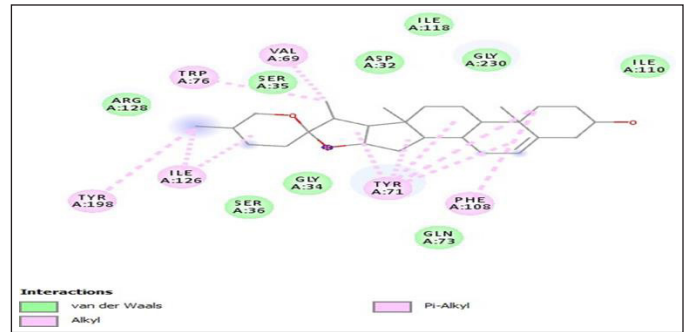


Figure 3. 2-D interaction docking model of BACE 1 against DG.

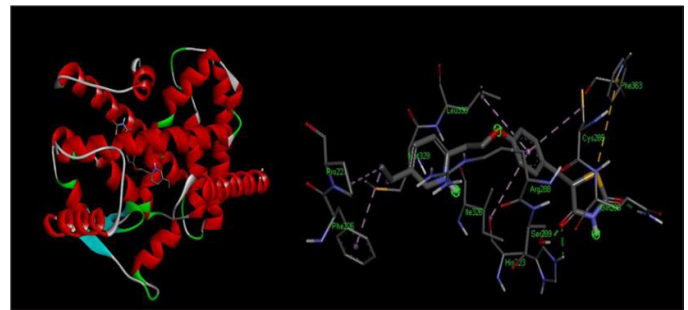


Figure 4. Pioglitazone interaction with 3-D crystallographic structure of PPAR- $\gamma$ .

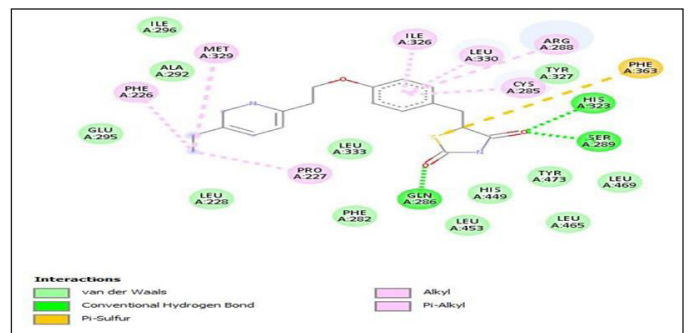


Figure 5. 2-D interaction of protein PPAR- $\gamma$  against Pioglitazone.

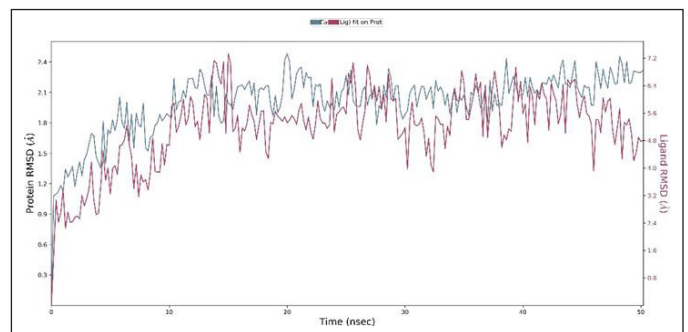


Figure 6. RMSD (Å) of the simulated BACE-1 and backbone atom with DG.

The MTT assay findings indicate that the tested substances, Pioglitazone as well as the combination of Pioglitazone with DG were noncytotoxic and cell-proliferative in nature on human neuroblastoma cells as it shows  $p < 0.001$  level of significance.

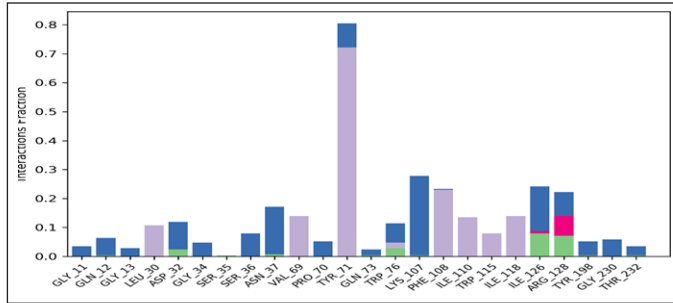


Figure 7. Represents the interaction of DG with enzyme BACE-1 during MD simulation.

Table 4. Details of drug treatment to respective cell lines used for the study.

S. No	Test compound	Cell line	Concentrations treated to cells
1	Untreated	SH-SY5Y	No treatment
2	Vehicle control	SH-SY5Y	0.1% DMSO
3	Blank	-	Only Media without cells
4	Std control	SH-SY5Y	10 $\mu$ M/ml
5	Test compounds—DG Pioglitazone	SH-SY5Y	5 (6.25, 12.5, 25, 50, 100 $\mu$ M/ml)

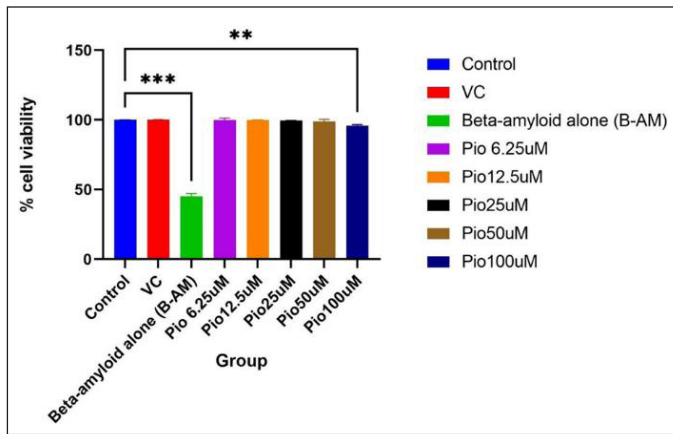


Figure 8. % Cell viability of PIO treated SH-SY5Y cell line.

Combination assay

This study examines the cytotoxicity of three chemicals on SH-SY5Y cells. The test chemicals that were utilized to treat the cells are listed in Table 5.

- According to MTT assay findings, the test chemical is cytotoxic viz.,  $A\beta$  protein fragment  $A\beta_{25-35}$  causing effective cytotoxicity on Human neuroblastoma (SH-Sy5Y) cells with  $IC_{50}$  values of 9.50  $\mu$ M/ml (10  $\mu$ M/ml) after the incubation period of 24 hours.
- In the  $A\beta$  neurotoxicity induced model, Pioglitazone (Fig. 11), DG (Fig. 12), and Pioglitazone + DG (1:1 ratio) (Fig. 13) compounds showed effective neuro-protective potency by recovering the cells death/autophagy on dose-dependent manner as it shows  $p < 0.001$  level of significance.

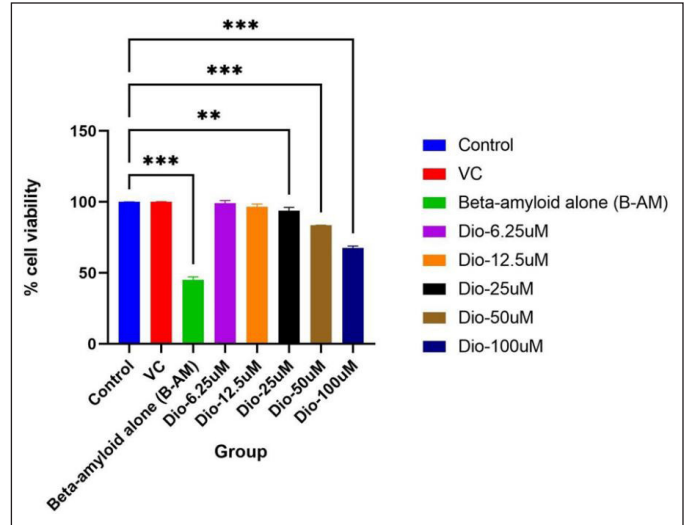


Figure 9. % Cell viability of DG treated SH-SY5Y cell line.

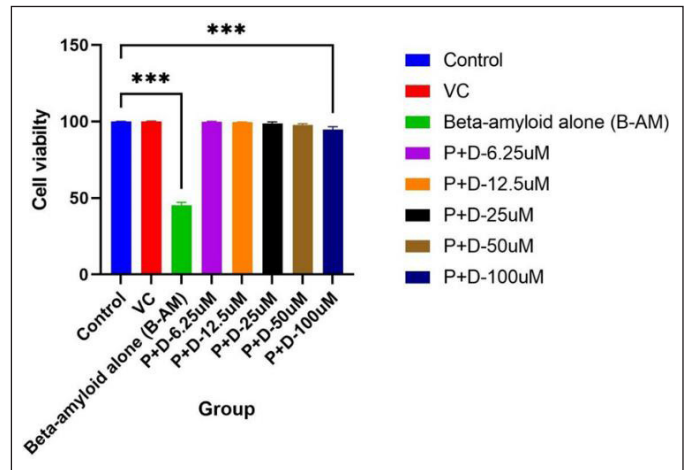


Figure 10. % Cell viability of PIO + DG treated SH-SY5Y cell line.

Table 5. Drug treatment in  $A\beta_{25-35}$  induced SH-SY5Y cell line.

S. No	Test compound	Cell line	Concentrations treated to cells
1	Untreated	SH-SY5Y	No treatment
2	Vehicle control	SH-SY5Y	0.1% DMSO
3	Blank	-	Only Media without cells
4	Std control	SH-SY5Y	10 $\mu$ M/ml
5	Test compounds	SH-SY5Y cells stimulated with B-AM	5 (6.25, 12.5, 25, 50, 100 $\mu$ M/ml)

The % cell viability of SH-SY5Y cell line along with  $IC_{50}$  and optimum concentration and morphological observation of SH-SY5Y cell line after 24 hours. of MTT assay was shown in Figures 14 and 15, respectively.

ROS assay

To measure the ROS expression of given test compounds on  $A\beta$  induced SHSY-5Y flow cytometry staining

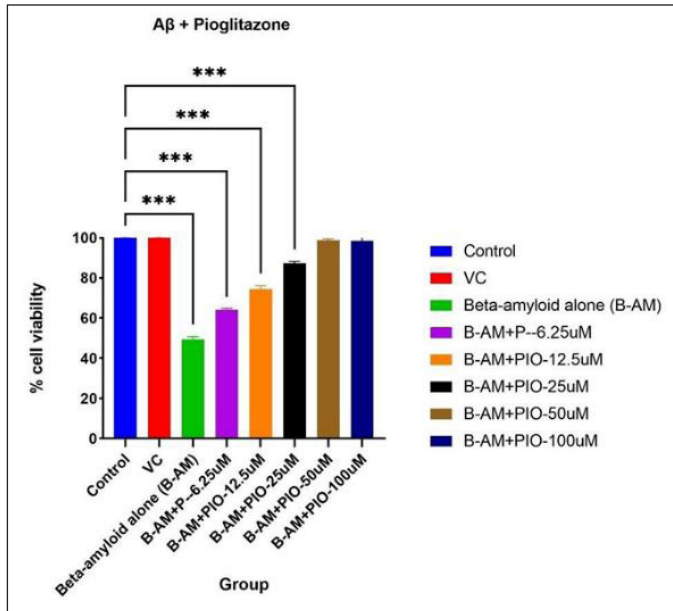


Figure 11. % Cell viability of Aβ<sub>25-35</sub> + PIO treated SH-SY5Y cell line.

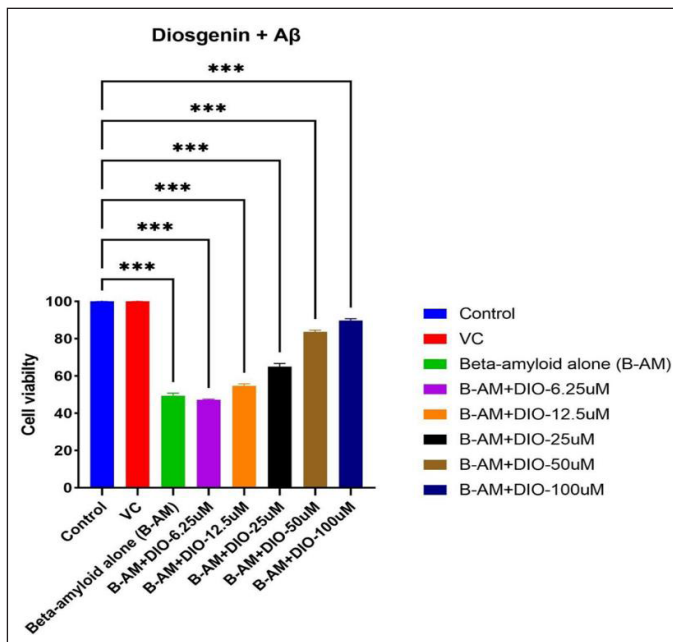


Figure 12. % Cell viability of Aβ<sub>25-35</sub> + DG treated SH-SY5Y cell line.

of cell lines with H2DCFDA. The sample details are mentioned in Table 6.

**Observation**

H2DCFDA expression study of the test compounds against Aβ induced SH-SY5Y cell line was shown in Table 7 and the results were presented in Figure 16.

The gated SH-SY5Y singlets' H2DCFDA histograms discriminate between M1 and M2 phase cells. A negative expression/region is designated as M1, while a positive expression/region is designated as M2. It is possible to fine-tune

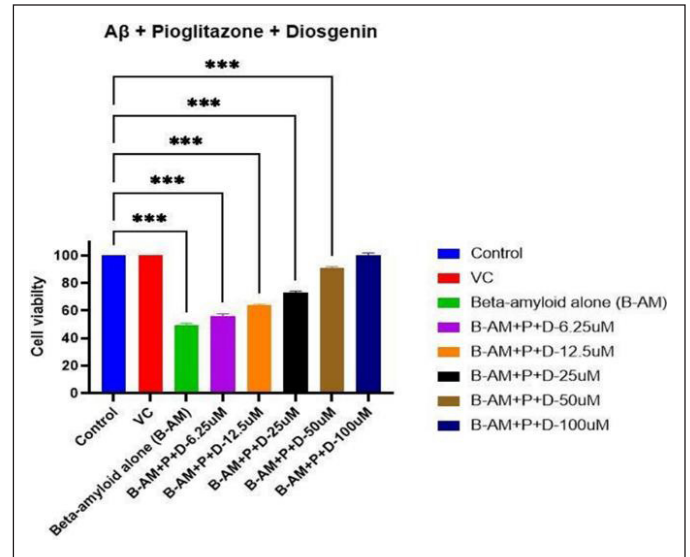


Figure 13. % Cell viability of Aβ<sub>25-35</sub> + PIO + DG treated SH-SY5Y cell line.

the gating of the M1 and M2 phases using software analysis (Cell Quest Software, Version 6.0).

Pioglitazone, DG, and their combination treated cells significantly suppressed the DCF expression in Aβ induced model as compared to Aβ alone treated cells (Fig. 17). For the ROS study, the minimum concentration of the tested drugs that significantly reduced Aβ toxicity by showing more than 85%–90% cell survival was taken into account.

When compared to Aβ-induced cells, a 25 μM/ml dose of Pioglitazone produced a satisfactory reduction in DCF intensity, but DG at a dose of 50 μM/ml showed a moderate suppression of DCF intensity. DCF expression was seen in 56.49% of Aβ-induced cells and 13.8% of cells treated with Aβ plus Pioglitazone and DG, respectively.

Overall, the results showed that the given compounds, Pioglitazone and DG, have neuroprotective potential since they greatly reduced the oxidative stress-induced apoptosis caused by Aβ, as determined by measuring DCF intensity.

**ELISA**

Inflammatory cytokine levels will be significantly increased in AD. In ELISA, the expression of IL 1β and TNF α markers is measured.

TNF-α and IL-1β levels were measured using ELISA in Aβ<sub>25-35</sub> induced SHSY5Y cell line models treated with different concentrations of Pioglitazone, DG, or a combination of both (3.125, 6.25, 12.12.5, and 25 M). When the maximum concentration (25 M) was used, the levels of TNF- and IL-1 were significantly reduced (Figs. 18 and 19–21).

**Discussion**

This study was designed to determine whether the novel combination of Pioglitazone and DG can successfully inhibit the toxicity caused by Aβ<sub>25-35</sub> in human neuroblastoma cells (SH-SY5Y). We hypothesized that this novel combination could alleviate the toxicity caused by Aβ<sub>25-35</sub> peptide based on the finding that DG significantly reduced the cerebral

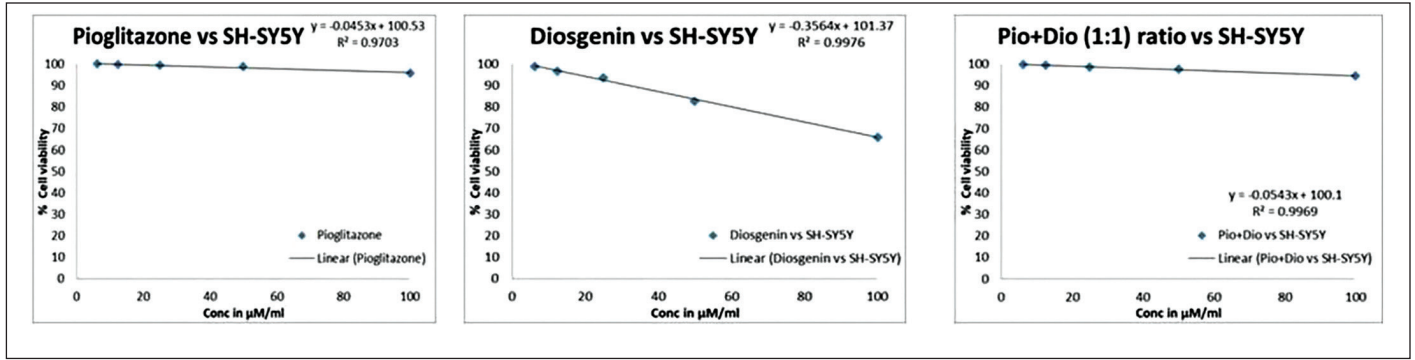


Figure 14. % Cell viability of SH-SY5Y cell line along with IC<sub>50</sub> and optimum concentration.

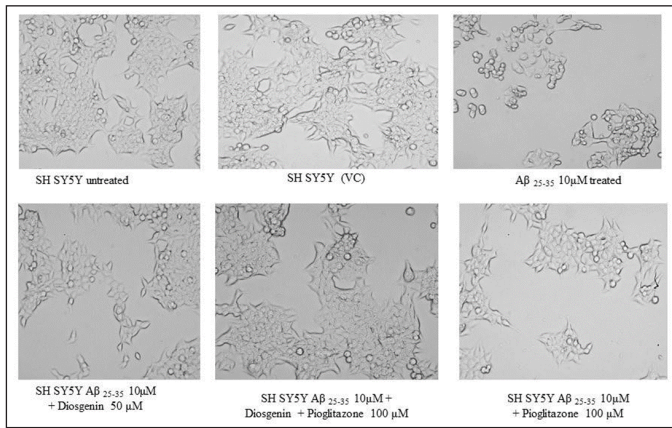


Figure 15. Morphological observation of SH-SY5Y cell line after 24 hrs. of MTT.

Table 6. Details of samples used for the study.

S. No.	Sample name/code	Concentrations used for the study	Cell line
1	Untreated	-	SH-SY5Y
2	Aβ alone	10 μM/ml	SH-SY5Y
3	Aβ + Pio	10 μM/ml + 25 μM/ml	SH-SY5Y
4	Aβ + Dio	10 μM/ml + 50 μM/ml	SH-SY5Y
5	Aβ + {Pio+Dio}	10 μM/ml + 50 μM/ml	SH-SY5Y

Table 7. H2DCFDA expression study of the test compounds against SH-SY5Y cell line.

Culture condition	% Cells expressed DCF intensity ±SD (N = 3)
Untreated	0.56 ± 0.40
Aβ – 10 uM alone	57.59 ± 1.33
Aβ + Pio	22.51 ± 2.96
Aβ + Dio	31.87 ± 2.94
Aβ + Dio + Pio	15.26 ± 1.49

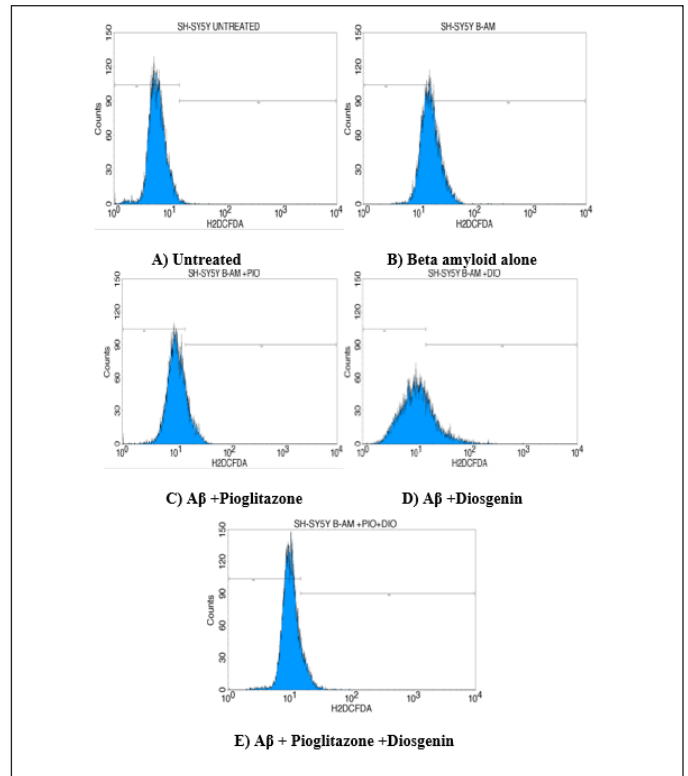


Figure 16. H2DCFDA expression study of untreated (A), Aβ alone with 10 μM/ml (B), Aβ + Pioglitazone-25 μM/ml (C), Aβ + DG-50 μM/ml (D), and Aβ + Pioglitazone + DG-50 μM/ml (E) concentrations against the SH-SY5Y cells using BD FACS Calibur, Cell Quest Pro Software (Version 6.0).

cortex and hippocampal deposition of Aβ plaques and NFTs [38] and PPAR-γ agonists have anti-inflammatory properties, regulate Aβ homeostasis, and have neuroprotective potential [39]. Whilst this is only a hypothesis at this point, there is currently no concrete experimental evidence to support how well this combination would affect neurotoxicity and morphological deterioration. Thus, to evaluate whether DG and Pio individually and in combination have a beneficial effect on neurotoxicity, we intoxicated Aβ<sub>25-35</sub> peptide in SH-SY5Y cells.



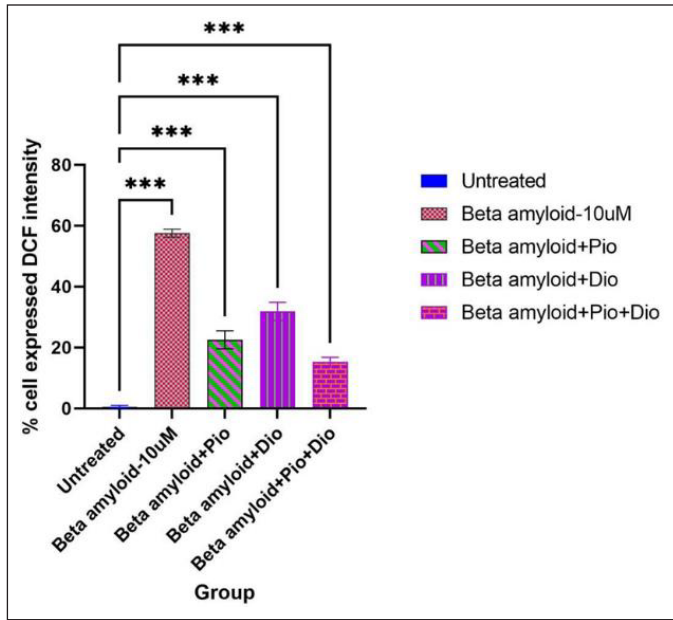


Figure 17. ROS Expression in SH-SY5Y Aβ<sub>25-35</sub> induced model.

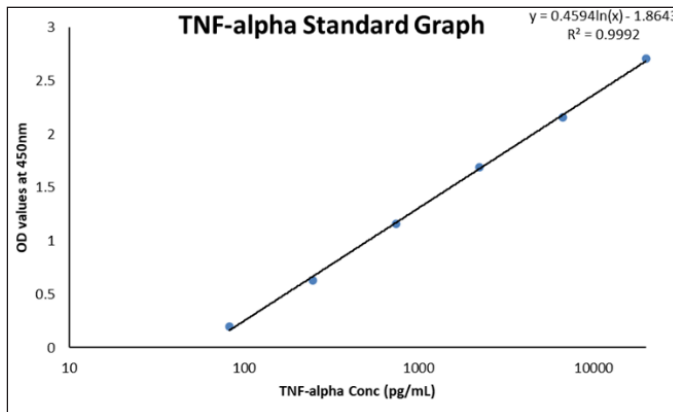


Figure 18. TNF-α standard Graph.

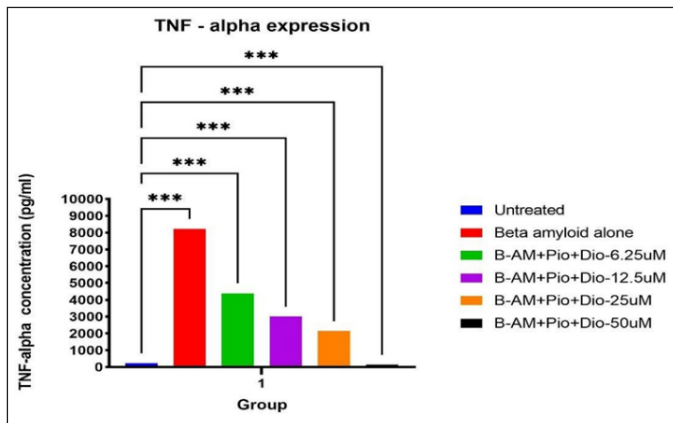


Figure 19. TNF-α Expression in SHSY5Y cell line model.

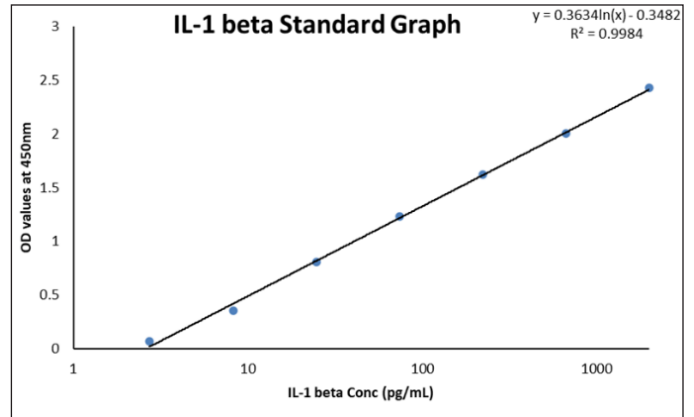


Figure 20. IL-1β standard Graph.

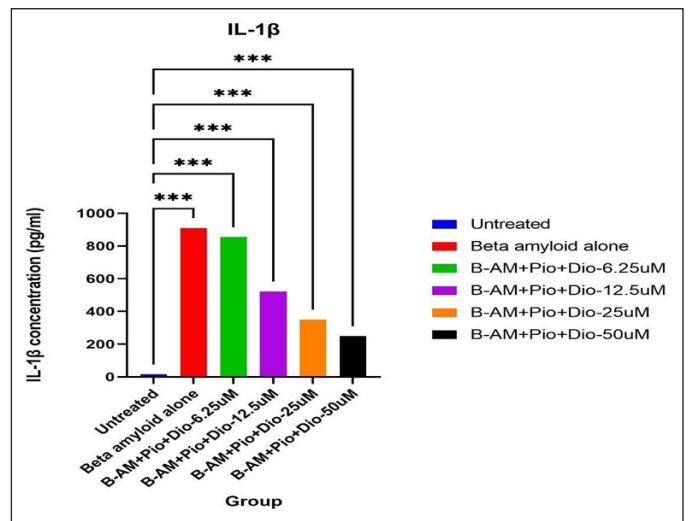


Figure 21. IL-1β Expression in SH-SY5Y cell line model.

*In silico* studies have revealed that the natural substance DG has good BBB penetration, which ensures that the drug will actively reach the brain and exert its effect by binding to BACE-1 enzyme.

The MTT assay determines the mitochondrial redox potential of live cells, in this context SH-SY5Y cells, and therefore measures changes in color of the redox dye from yellow to purple or blue in healthy cells as opposed to unhealthy cells. According to previous literature reporting that Aβ<sub>25-35</sub> inhibits the cellular reduction of MTT, the MTT redox levels were lowered in the Aβ<sub>25-35</sub> treated SH-SY5Y cells [40]. Considering it a measure of cell viability, the percentage reduction of MTT was discovered to be much higher in Aβ<sub>25-35</sub> + PIO + DG treated cells than in cells treated with Aβ<sub>25-35</sub> alone, suggesting that this combination is responsible for the enhanced redox activity in these cells.

The ROS assay is a cell-based approach to assess the activity of hydroxyl, peroxyl, and other reactive oxygen species.

Measuring DCF intensity revealed that both Pioglitazone and DG greatly reduced the oxidative stress-induced apoptosis induced by A $\beta$ . In A $\beta$ -induced SH-SY5Y cells, the combination of Pio and Dio in a 1:1 ratio produced better inhibition of DCF intensity than the individual drugs.

Both experimental and clinical data have shown that the AD brain produces more proinflammatory cytokines, such as TNF- $\alpha$ , IFN- $\gamma$ , IL-1 $\beta$ , IL-6, and IL-18, and that their receptors are upregulated during the disease progression [41]. Tau hyperphosphorylation and neuronal death are caused by pro-inflammatory cytokines, such as TNF- $\alpha$ , IL-1 $\beta$ , IL-6, and IL-18, that are elevated as a result of A $\beta$  binding to the surface of microglial cells [42]. Earlier studies also revealed that transcript levels for several proinflammatory markers, specifically TNF- $\alpha$  and IL-1 $\beta$ , were increased in AD, specifically in response to tau [43]. Therefore, in the current study, TNF- $\alpha$  and IL-1 $\beta$  levels were measured using ELISA, and it was found that these levels were significantly lowered when the cells were treated with Pioglitazone (PIO) and DG together, indicating that these drugs have a significant protective role for the cells against neuroinflammation.

## CONCLUSION

The effectiveness of all AD therapeutic interventions is confined. Currently, symptomatic improvement over pretreatment baseline constitutes the best short-term outcome. The reliability of combination therapy has, therefore, been considered to be important due to the availability of drugs for the treatment of AD that have diverse mechanisms of action. Two potential treatments for AD include cholinesterase inhibitors and N-methyl-D-aspartate antagonists, both of which have a lengthy history of usage in clinical settings. Due to their poor therapeutic efficacy, these drugs have not been successful at eliminating A $\beta$  plaque, NFTs, or improving cognitive function. In the current study, we evaluated both individual and combined neuroprotective effects of DG and Pioglitazone in AD. The study found that the combined effects of these medications showed more significant neuroprotection than their individual effects. Pioglitazone, which suppresses nuclear factor kappa B via activating PGC-1, and DG, which is observed to inhibit the BACE-1 enzyme and promote A $\beta$  clearance, together decreased neuroinflammation and the growth of A $\beta$  plaque.

We could, therefore, conclude by stating that Pioglitazone and DG together may be a promising novel neuroprotective combination for neurodegenerative disorders like Alzheimer's. However, it is crucial to carry out *in vivo* and clinical investigations to understand more about the underlying neuroprotective mechanism of these drugs as well as regarding their toxicity or side effects associated with their long-term usage.

## AUTHOR CONTRIBUTIONS

All authors made substantial contributions to conception and design, acquisition of data, or analysis and interpretation of data; took part in drafting the article or revising it critically for important intellectual content; agreed to submit to the current journal; gave final approval of the version to be

published; and agree to be accountable for all aspects of the work. All the authors are eligible to be an author as per the international committee of medical journal editors (ICMJE) requirements/guidelines.

## FINANCIAL SUPPORT

There is no funding to report.

## CONFLICTS OF INTEREST

The authors report no financial or any other conflicts of interest in this work.

## ETHICAL APPROVALS

This study does not involve experiments on animals or human subjects.

## DATA AVAILABILITY

All data generated and analyzed are included in this research article.

## PUBLISHER'S NOTE

This journal remains neutral with regard to jurisdictional claims in published institutional affiliation.

## REFERENCES

1. Tam JHK, Pasternak SH. Alzheimer's disease. In: The cerebral cortex in neurodegenerative and neuropsychiatric disorders: experimental approaches to clinical issues. Elsevier Inc.; 2017. pp 83–118.
2. Rajmohan R, Reddy PH. Amyloid-beta and phosphorylated tau accumulations cause abnormalities at synapses of Alzheimer's disease neurons. *J Alzheimers Dis.* 2017;57(4):975–99.
3. Burns A, Iliffe S. Alzheimer's disease. *BMJ.* 2009;338:b158.
4. Ballard C, Mobley W, Hardy J, Williams G, Corbett A. Dementia in Down's syndrome. *Lancet Neurol.* 2016 May;15(6):622–36.
5. Lammich S, Kojro E, Postina R, Gilbert S, Pfeiffer R, Jasionowski M, *et al.* Constitutive and regulated-secretase cleavage of Alzheimer's amyloid precursor protein by a disintegrin metalloprotease. [Internet]. *Proc Natl Acad Sci U S A.* 1999 Mar 30;96(7):3922–7. Available from: [www.pnas.org](http://www.pnas.org)
6. Lin X, Koelsch G, Wu S, Downs D, Dashti A, Tang J. Human aspartic protease memapsin 2 cleaves the beta-secretase site of beta-amyloid precursor protein. *Proc Natl Acad Sci U S A.* 2000 Feb 15;97(4):1456–60.
7. Sisodia SS, St George-Hyslop PH. Gamma-secretase, notch, abeta and Alzheimer's disease: where do the presenilins fit in? *Nat Rev Neurosci.* 2002 Apr;3(4):281–90.
8. Atwood CS, Bowen RL. A unified hypothesis of early- and late-onset Alzheimer's disease pathogenesis. *J Alzheimers Dis* [Internet]. 2015 Jul;47(1):33–47. doi: <https://doi.org/10.3233%2Fjad-143210>
9. Citron M, Vigo-Pelfrey C, Teplow DB, Miller C, Schenk D, Johnston J, *et al.* Excessive production of amyloid beta-protein by peripheral cells of symptomatic and presymptomatic patients carrying the Swedish familial Alzheimer disease mutation. *Proc Natl Acad Sci* [Internet]. 1994 Dec;91(25):11993–7. doi: <https://doi.org/10.1073%2Fpnas.91.25.11993>
10. Justin A, Mandal S, Prabitha P, Dhivya S, Yuvaraj S, Kabadi P, *et al.* Rational design, synthesis, and *in vitro* neuroprotective evaluation of novel glitazones for PGC-1 $\alpha$  activation via PPAR- $\gamma$ : a new therapeutic strategy for neurodegenerative disorders. *Neurotox Res.* 2020;37(3):508–24.
11. Sethi G, Shanmugam MK, Warriar S, Merarchi M, Arfuso F, Kumar AP, *et al.* Pro-apoptotic and anti-cancer properties of Diosgenin: a comprehensive and critical review. *Nutrients.* 2018;10:645.

12. Chiang SS, Chang SP, Pan TM. Osteoprotective effect of monascus-fermented *Dioscorea* in ovariectomized rat model of postmenopausal osteoporosis. *J Agric Food Chem*. 2011;59(17):9150–7.
13. Jesus M, Martins APJ, Gallardo E, Silvestre S. Diosgenin: recent highlights on pharmacology and analytical methodology. *J Anal Methods Chem*. 2016;2016:4156293.
14. Lv YC, Yang J, Yao F, Xie W, Tang YY, Ouyang XP, *et al.* Diosgenin inhibits atherosclerosis via suppressing the MiR-19b-induced downregulation of ATP-binding cassette transporter A1. *Atherosclerosis*. 2015 May;240(1):80–9.
15. Hua S, Li Y, Su L, Liu X. Diosgenin ameliorates gestational diabetes through inhibition of sterol regulatory element-binding protein-1. *Biomed Pharmacother*. 2016;84:1460–5.
16. Kim JE, Go J, Koh EK, Song SH, Sung JE, Lee HA, *et al.* Diosgenin effectively suppresses skin inflammation induced by phthalic anhydride in IL-4/Luc/CNS-1 transgenic mice. *Biosci Biotechnol Biochem*. 2016;80(5):891–901.
17. Blunden G, Rhodes CT. Stability of Diosgenin. *J Pharm Sci* [Internet]. 1968 Apr;57(4):602–4. doi: <https://doi.org/10.1002%2Fjps.2600570411>
18. Okawara M, Hashimoto F, Todo H, Sugibayashi K, Tokudome Y. Effect of liquid crystals with cyclodextrin on the bioavailability of a poorly water-soluble compound, Diosgenin, after its oral administration to rats. *Int J Pharm*. 2014;472(1–2):257–61.
19. Fu WY, Wang X, Ip NY. Targeting neuroinflammation as a therapeutic strategy for Alzheimer's disease: mechanisms, drug candidates, and new opportunities. *ACS Chem Neurosci*. 2019;10:872–9.
20. Wang S, Wang F, Yang H, Li R, Guo H, Hu L. Diosgenin glucoside provides neuroprotection by regulating microglial M1 polarization. *Int Immunopharmacol*. 2017;50:22–9.
21. Tohda C, Lee YA, Goto Y, Nemere I. Diosgenin-induced cognitive enhancement in normal mice is mediated by 1,25D 3-MARRS. *Sci Rep*. 2013;3:3395.
22. Tohda C, Yang X, Matsui M, Inada Y, Kadomoto E, Nakada S, *et al.* Diosgenin-rich yam extract enhances cognitive function: a placebo-controlled, randomized, double-blind, crossover study of healthy adults. *Nutrients*. 2017;9(10):1160.
23. Som S, Antony J, Dhanabal SP, Ponnusankar S. Neuroprotective role of Diosgenin, a NGF stimulator, against A (142) induced neurotoxicity in animal model of Alzheimer's disease. *Metab Brain Dis* [Internet]. 2022 Jan;37(2):359–72. doi: <https://doi.org/10.1007%2Fs11011-021-00880-8>
24. Qin Y, Wu X, Huang W, Gong G, Li D, He Y, *et al.* Acute toxicity and sub-chronic toxicity of steroidal saponins from *Dioscorea zingiberensis* C. H. Wright in rodents. *J Ethnopharmacol* [Internet]. 2009 Dec;126(3):543–50. doi: <https://doi.org/10.1016%2Fj.jep.2009.08.047>
25. Peila R, Rodriguez BL, Launer LJ. Type 2 diabetes, APOE gene, and the risk for dementia and related pathologies: the Honolulu-Asia aging study. *Diabetes*. 2002;51(4):1256–62.
26. Craft S, Watson GS. Insulin and neurodegenerative disease: shared and specific mechanisms. *Lancet Neurol*. 2004;3:169–78.
27. Landreth G. Therapeutic use of agonists of the nuclear receptor PPARgamma in Alzheimer's disease. *Curr Alzheimer Res*. 2007;4(2):159–64.
28. Pa P, Justin A, Ananda Kumar TD, Chinaswamy M, Kumar BRP. Glitazones activate PGC-1 $\alpha$  signaling via PPAR- $\gamma$ : a promising strategy for antiparkinsonism therapeutics. *ACS Chem Neurosci*. 2021;12:2261–72.
29. Egan WJ, Kenneth M. Merz, Baldwin JJ. Prediction of drug absorption using multivariate statistics. *J Med Chem* [Internet]. 2000 Sep;43(21):3867–77. doi: <https://doi.org/10.1021%2Fjm000292e>
30. Sabe VT, Ntombela T, Jhamba LA, Maguire GEM, Govender T, Naicker T, *et al.* Current trends in computer aided drug design and a highlight of drugs discovered via computational techniques: a review. *Eur J Med Chem* [Internet]. 2021 Nov;224:113705. doi: <https://doi.org/10.1016%2Fj.ejmech.2021.113705>
31. Stanzione F, Giangreco I, Cole JC. Use of molecular docking computational tools in drug discovery. In: *Progress in medicinal chemistry* [Internet]. Elsevier; 2021. pp 273–343. doi: <https://doi.org/10.1016%2Fbs.pmch.2021.01.004>
32. Bowers KJ, Sacerdoti FD, Salmon JK, Shan Y, Shaw DE, Chow E, *et al.* Molecular dynamics—scalable algorithms for molecular dynamics simulations on commodity clusters. In: *Proceedings of the 2006 ACM/IEEE Conference on Supercomputing—SC 06* [Internet]. ACM Press; 2006. doi: <https://doi.org/10.1145%2F1188455.1188544>
33. Jorgensen WL, Chandrasekhar J, Madura JD, Impey RW, Klein ML. Comparison of simple potential functions for simulating liquid water. *J Chem Phys* [Internet]. 1983 Jul;79(2):926–35. doi: <https://doi.org/10.1063%2F1.445869>
34. Jupudi S, Rajagopal K, Murugesan S, Kumar BK, Raman K, Byran G, *et al.* Identification of papain-like protease inhibitors of SARS CoV-2 through HTVS, molecular docking, MMGBSA and molecular dynamics approach. *South Afr J Botany* [Internet]. 2022 Dec;151:82–91. doi: <https://doi.org/10.1016%2Fj.sajb.2021.11.033>
35. Pike CJ, Burdick D, Walencewicz AJ, Glabe CG, Cotman CW. Neurodegeneration induced by beta-amyloid peptides *in vitro*: the role of peptide assembly state. *J Neurosci* [Internet]. 1993 Apr;13(4):1676–87. doi: <https://doi.org/10.1523%2Fjneurosci.13-04-01676.1993>
36. Wang X, Zhang M, Liu H. LncRNA17A regulates autophagy and apoptosis of SH-SY5Y cell line as an *in vitro*/model for Alzheimer's disease. *Biosci Biotechnol Biochem* [Internet]. 2019 Apr;83(4):609–21. doi: <https://doi.org/10.1080%2F09168451.2018.1562874>
37. Mairuae N, Connor JR, Lee SY, Cheepsunthorn P, Tongjaroenbuangam W. The effects of okra (*Abelmoschus esculentus* Linn.) on the cellular events associated with Alzheimer's disease in a stably expressed HFE neuroblastoma SH-SY5Y cell line. *Neurosci Lett* [Internet]. 2015 Aug;603:6–11. doi: <https://doi.org/10.1016%2Fj.neulet.2015.07.011>
38. Lecanu L, Yao W, Teper GL, Yao ZX, Greeson J, Papadopoulos V. Identification of naturally occurring spirostenols preventing  $\beta$ -amyloid-induced neurotoxicity. *Steroids*. 2004;69(1):1–16.
39. Jiang Q, Heneka M, Landreth GE. The role of peroxisome proliferator-activated receptor- $\gamma$  (PPAR $\gamma$ ) in Alzheimer's disease: therapeutic implications. *CNS Drugs*. 2008;22:1–14.
40. Shearman MS, Hawtin SR, Tailor VJ. The intracellular component of cellular 3-(4,5-dimethylthiazol-2-yl)-2,5-diphenyltetrazolium bromide (MTT) reduction is specifically inhibited by  $\beta$ -amyloid peptides. *J Neurochem*. 1995;65(1):218–27.
41. Sastre M, Klockgether T, Heneka MT. Contribution of inflammatory processes to Alzheimer's disease: molecular mechanisms. *Int J Dev Neurosci*. 2006;24:167–76.
42. von Bernhardi R, Tichauer JE, Eugenin J. Aging-dependent changes of microglial cells and their relevance for neurodegenerative disorders. *J Neurochem*. 2010;112:1099–114.
43. Wang DB, Dayton RD, Zweig RM, Klein RL. Transcriptome analysis of a tau overexpression model in rats implicates an early pro-inflammatory response. *Exp Neurol*. 2010;224(1):197–206.

**How to cite this article:**

Mohammed S, Nandhyala A, Gaddam NR, Rajagopal K, Palathoti N, Antony J. Preliminary screening of Pioglitazone and Diosgenin novel combination for Alzheimer's disease. *J Appl Pharm Sci*. 2023;13(Suppl 1):065–075.